RSC Advances

PAPER

View Article Online
View Journal | View Issue

Cite this: *RSC Adv.*, 2024, **14**, 36264

Developing $Ni_{0.5}Zn_{0.5}Fe_2O_4$ ferrite with controlled particle size and morphology through optimized processing conditions of low energy solid state reaction†

Sarah Baayyad,[a] Fatima-Zahra Semlali,[a] El Kébir Hlil,[c] Tarik Mahfoud,[b] Hassan El Moussaoui*[b] and Mounir El Achaby*[a]

Received 1st October 2024
Accepted 30th October 2024

DOI: 10.1039/d4ra07076c

rsc.li/rsc-advances

Soft magnetic materials, like $Ni_{0.5}Zn_{0.5}Fe_2O_4$, require high temperatures and regulated environments for their manufacture and processing, which can be highly energy intensive. These requirements therefore result in higher production costs and energy consumption. To address this issue, the development of composite materials based on soft magnetic ferrites has become a prominent research area. The type of particles and their size distribution, shape, and dispersion within the polymer matrix can be crucial for controlling the magnetic properties. In this context, and to reduce energy consumption, the parameters of solid-state reaction (such as calcination temperature, calcination time, and milling time) were optimized in this work to produce magnetic particles with suitable shape and size for filling a thermoplastic matrix. The impact of these parameters on phase purity, morphology, particle size, and magnetic properties was thoroughly evaluated. The results highlight that the sample synthesized at 1200 °C for 6 hours achieved an impressive saturation magnetization value of 80.07 emu g^{-1}, showcasing exceptional magnetic performance.

1. Introduction

The rapid development of modern electronic devices, telecommunication systems, and other technological applications has generated an increasing demand for soft magnetic materials with superior properties.[1] These materials are essential components in a wide range of applications, from transformers and inductors to electromagnetic wave absorbers.[2,3] Also they are great materials to overcome electromagnetic issues.[4] Among soft magnetic materials, ferrites have emerged as highly attractive candidates due to their unique combination of properties, including high electrical resistivity, low eddy current losses, mechanical hardness, and good magnetic saturation. Nickel zinc ferrite ($Ni_{0.5}Zn_{0.5}Fe_2O_4$) stands out as a particularly interesting soft magnetic material due to its tunable magnetic properties, making it suitable for high-frequency applications.[5] Moreover, the doping of $NiFe_2O_4$ by non-magnetic Zn results in the modification of the AB_2O_4-type of crystal structure by cation redistribution in the crystal lattice as well as changes in the microstructure and magnetic and electric properties. The above mentioned properties can be controlled and are strictly dependent on the amount of Zn content and the type of synthesis procedure.[6] Ni–Zn ferrite is a spinel structure in which tetrahedral A sites are occupied by Zn^{2+} and Fe^{3+} ions and octahedral B sites by Ni^{2+} and Fe^{3+} ions in the spinel formula AB_2O_4.[7] Magnetic properties of these ferrites are mainly controlled by the cation distribution of Ni, Zn and Fe along the available tetrahedral and octahedral sites.[8] In the $Ni_{x-1}Zn_{x-1}Fe_2O_4$ system, $Ni_{0.5}Zn_{0.5}Fe_2O_4$ has the best magnetic characteristics and microwave absorption ability, and it is a suitable candidate for several applications, it possesses beneficial characteristics such as high dielectric constant, low dielectric loss, mechanical hardness, electrical resistivity, and chemical stability.[9,10] Ni–Zn ferrite is usually synthesized by the sol–gel methods,[11–13] co-precipitation methods,[14,15] combustion method[16,17] and hydrothermal synthesis.[18,19] One of the most used methods for synthesizing ferrite magnetic particles is the solid-state reaction. This technique of processing ferrite materials often involves high temperatures and controlled atmospheres, making the production process energy-intensive and costly. The sintering or calcination process, which is crucial for achieving phase purity and optimal magnetic properties,

[a]*Materials Science, Energy and Nanoengineering Department (MSN), Mohammed VI Polytechnic University (UM6P), Lot 660 – Hay Moulay Rachid, Ben Guerir, 43150, Morocco. E-mail: mounir.elachaby@um6p.ma*

[b]*Moroccan Foundation for Advanced Science, Innovation and Research (MAScIR), Rabat Design Center, Rue Mohamed El Jazouli, Madinat El Irfane, 10100 Rabat, Morocco. E-mail: h.elmoussaoui@mascir.ma*

[c]*Institut Néel, CNRS et Université Joseph Fourier, BP 166, F-38042 Grenoble Cedex 9, France*

† Electronic supplementary information (ESI) available. See DOI: https://doi.org/10.1039/d4ra07076c

typically occurs at elevated temperatures and requires extended durations.[20–22] Furthermore, the mechanical and chemical characteristics of the final product are highly dependent on the precise control of the processing parameters, such as calcination time, particle size, and morphology. These challenges highlight the need for optimizing synthesis processes that can reduce energy consumption. To address the issue of high energy consumption, research has increasingly focused on developing composite materials based on soft magnetic ferrites, particularly by incorporating magnetic particles like $Ni_{0.5}Zn_{0.5}Fe_2O_4$ into polymer matrices. This approach combines the lightweight, flexible, and corrosion-resistant properties of polymers with the enhanced mechanical, thermal, and magnetic properties of ferrites.[23,24] A key challenge is ensuring homogeneous distribution of magnetic particles within the polymer matrix, as particle size, shape, and dispersion greatly influence the composite's overall performance. This work aims to give researchers a clear guide to optimizing key synthesis parameters of low-energy solid-state reactions for producing polymer-magnetic composites with controlled magnetic properties. The study highlights how parameters like temperature, particle size, and calcination time impact the structural, morphological, and magnetic characteristics of the materials. This approach not only enhances the performance and functionality of polymer-based magnetic composites but also supports efficient and scalable manufacturing in this field.

2. Material and methods

A mixture of high purity commercial oxides powders, nickel oxide, zinc oxide and iron oxide, used as starting materials to prepare $Ni_{0.5}Zn_{0.5}Fe_2O_4$. The processes start with mixing the precursor using Agate vials and balls for the milling process in high energy planetary mill Pulverisette 4 (Fritsch). The ball to powder mass ratio was 20 : 1. The rotation speed was 500 rpm, with the variation of milling time from 30 min to 60 min. After milling, the samples were annealed in air at a temperature of 900 °C, 1000 °C, 1100 °C and 1200 °C, for 6 and 12 hours. Table 1 summarizes samples names and synthesis conditions.

Table 1 Samples names, milling condition, and treatment temperature and time

		Ball milling speed 500 (rpm)	Calcination conditions	
Sample's number	Samples	Time (min)	Temperature (°C)	Time (h)
1	NZF2C2B[a]	30	1200	6
2	NZFC12	30	1200	12
3	NZF-1-12	60	1200	12
4	NZF-1-6	60	1200	6
5	NZF1200	30	1200	6
6	NZF1100	30	1100	6
7	NZF1000	30	1000	6
8	NZF900	30	900	6

[a] NZF2C2B: this sample was subjected to double ball milling, each for 30 min, followed by a 6 hours calcination at 1200 °C.

The formation of spinel structure of $Ni_{0.5}Zn_{0.5}Fe_2O_4$ was investigated by D8-Discover diffractometer, Bruker (Nanotechnology Platform, MSN Laboratory). The CuK radiation (λ = 1.5418°) is used to scan the samples in the range of 5–80° with a step size of 0.01°, while the voltage and current are set at 45 kV and 100 mA, respectively.

The morphological properties of $NiZnFe_2O_4$ samples were investigated using a Zeiss EVO 10 scanning electron microscope (Carl Zeiss Microscopy, GmbH, Jena, Germany).

For magnetic properties High temperature extraction magnetometer BS1 (Louis Néel Magnetism Laboratory, CNRS, Grenoble) was used, with a resolution of 5×10^{-6}, and a temperature of 300 K to 800 K, and the field strength range is ±7 teslas.

3. Results and discussion

3.1. Processing information

Solid state reaction is a widely used industrial method for processing ceramic materials, including ferrite magnetic particles. This process involves several steps, such as ball milling for extended periods, pellet pressing, and multiple high-temperature, long duration calcinations. These steps make the process highly complex and energy intensive. To reduce the energy consumption during the processing of ferrite particles using solid state reaction, it is crucial to optimize reaction parameter, including ball milling time, calcination time, and temperature. The goal is to produce ferrite magnetic particles with a pure spinel phase, optimal stoichiometry, and a well-distributed size and shape of microparticles. Optimizing these parameters involves key adjustments. First, adjust the duration of ball milling to achieve a fine and homogeneous mixture without over-grinding. Adjusting the calcination parameters to ensure complete phase formation while minimizing energy usage. $Ni_{0.5}Zn_{0.5}Fe_2O_4$ is particularly advantageous due to its superior magnetic characteristics and microwave absorption ability, as well as its high dielectric constant, low dielectric loss, mechanical hardness, electrical resistivity, and chemical stability. These desirable properties make it an ideal candidate for synthesis *via* a low-energy solid state reaction. In this work, the approach involved synthesizing $Ni_{0.5}Zn_{0.5}Fe_2O_4$ using a low-energy solid state reaction. The initial step involved mixing the raw materials at a milling speed of 500 rpm for 30 min. This was followed by calcination at 1200 °C for 6 hours. After this calcination, an additional ball milling and calcination under the same condition were performed to study their effects on the purity of the phase and the shape and size of the particles. For the second sample, the same ball milling conditions were used, but the calcination duration was extended to 12 hours to study the effect of prolonged calcination on the magnetic particles. Additionally, the impact of mixing time on the properties of the particles was also investigated by increasing the ball milling time from 30 min to 60 min for both samples 3 and 4. The last parameter optimized in this study was the calcination temperature. The goal was to determine the minimum temperature

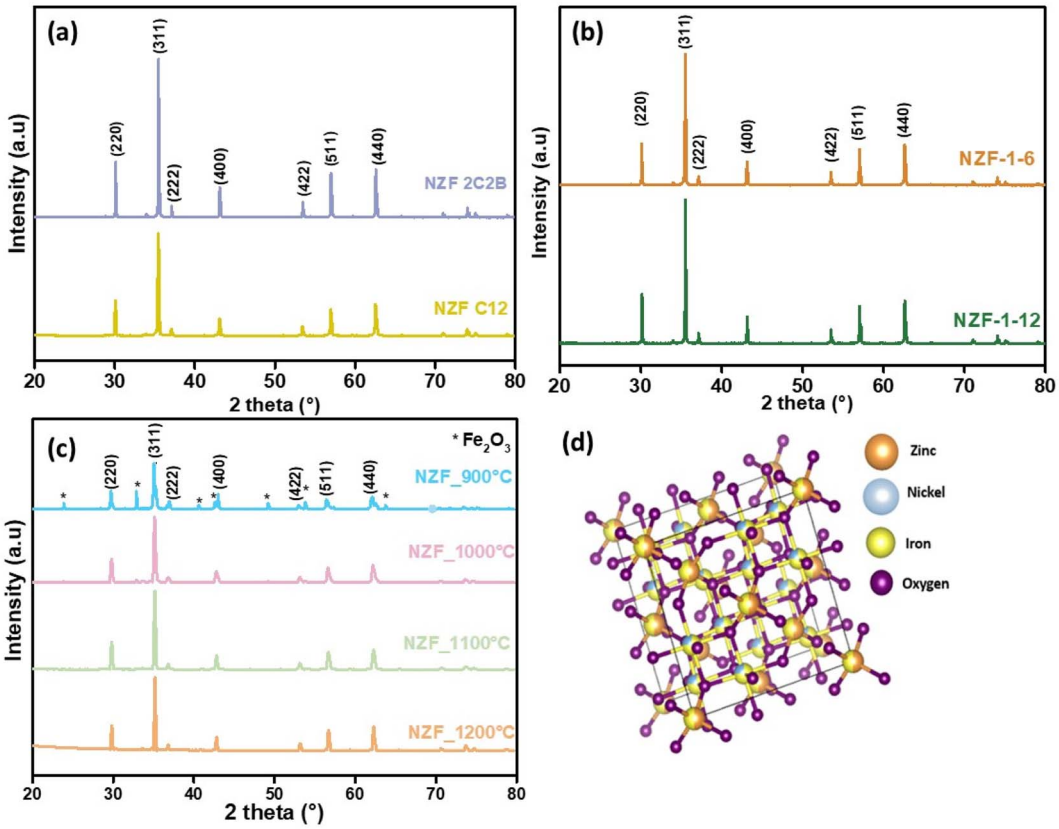

Fig. 1 XRD pattern of nickel zinc ferrite ($Ni_{0.5}Zn_{0.5}Fe_2O_4$) particles. (a) XRD pattern of NZFC12, NZF2C2B. (b) XRD pattern of NZF-1-6, and NZF-1-12. (c) XRD pattern of NZF900, NZF1000, NZF 1100, NZF1200. (d) The crystal structure of $Ni_{0.5}Zn_{0.5}Fe_2O_4$.

required to achieve a pure phase and good distribution of particle sizes. For samples 5, 6, 7, and 8, the calcination temperature was systematically decreased from the highest temperature of 1200 °C to 900 °C. Optimizing these parameters is crucial for producing ferrite magnetic particles with excellent magnetic properties and a well distributed particle size and shape. These optimized particles can be used as fillers in polymers matrices to produce homogenous polymer magnetic composite materials.

3.2. Structural characteristics

The phase purity of our samples depends on the reaction take place by diffusion, which depends directly on annealing time, temperature and mixing conditions.[25] So, it is necessary to modify these factors for good diffusion. The impact of annealing time on the purity of the crystalline structure was examined in Fig. 1a. In accordance with the joint committee on powder diffraction standards (JCPDS), the existence of (220), (311), (400), (422), (511), and (440) in XRD patterns is consistent with cubic structure. All the samples show a typical single-phase, without any impurity phases. Fig. 1b shows that varying the milling time from 30 min to 60 min did not have any noticeable effect on the structure purity. After examining the effect of calcination time and mixing on the purity of the structure, the effect of calcination temperature, which also significantly affects phase purity, was studied. The results for whole samples

Table 2 Crystalline properties of the synthesized spinel samples at different calcination, and ball milling conditions

Samples number	Samples name	Crystallite size (nm)	Lattice parameters (Å)	Volume of cell ($Å^3$)	X-ray density ($g\ cm^{-3}$)
1	NZF 2C2B	113.764	8.398	592.390	5.331
2	NZF C12	52.563	8.387	590.154	5.352
3	NZF-1-6	54.900	8.381	588.762	5.364
4	NZF-1-12	53.209	8.387	589.965	5.353
5	NZF 1200	33.730	8.388	590.351	5.350
6	NZF 1100	33.690	8.393	591.223	5.342
7	NZF 1000	33.660	8.396	592.043	5.335
8	NZF 900	33.608	8.412	595.379	5.305

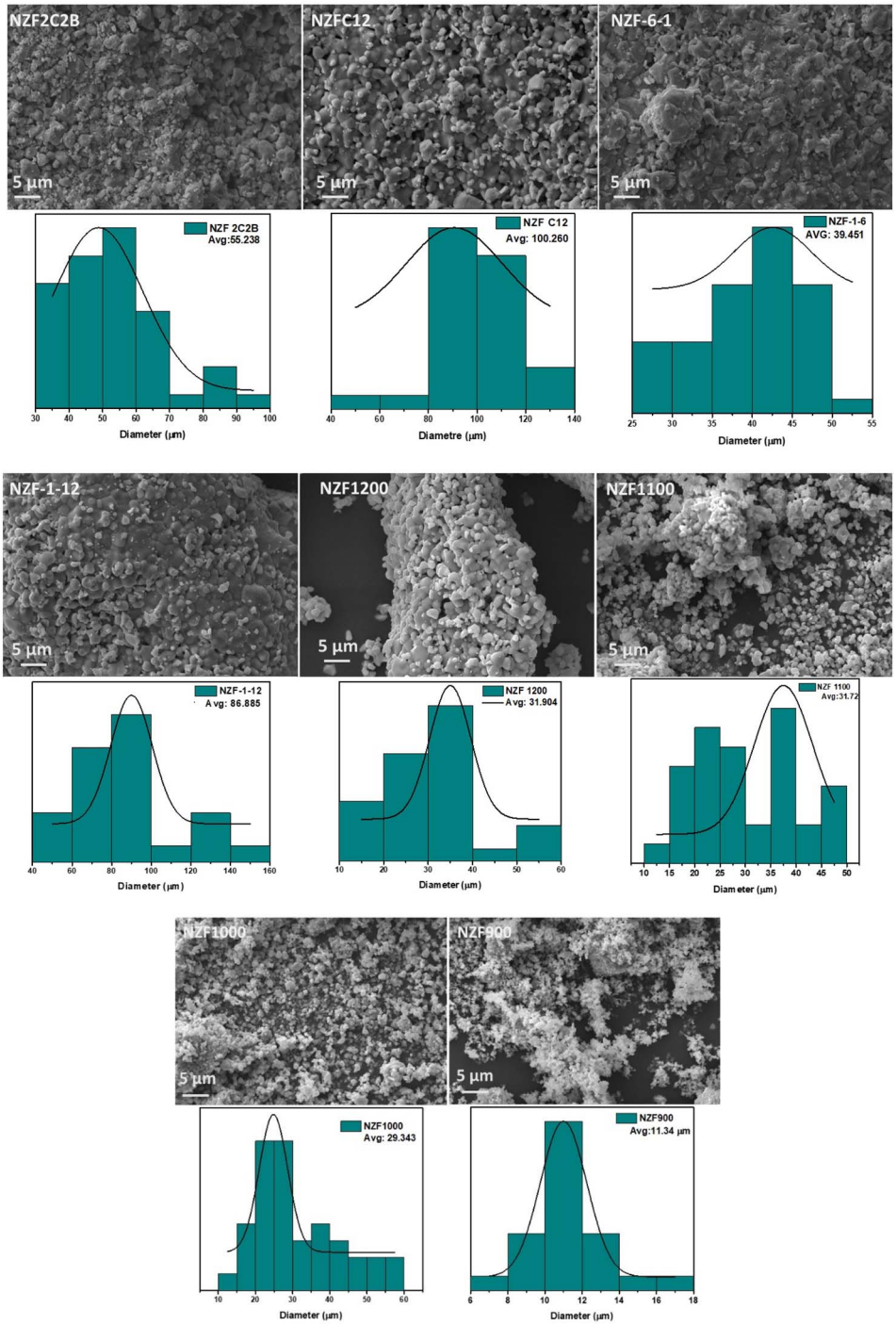

Fig. 2 SEM image and histogram of grain size distribution of all synthesized samples.

with temperature ranging from 900 to 1200 °C are shown in Fig. 1c. All the samples show a typical single-phase, without any impurity phases, except for NZF900, which show the formation of α-Fe_2O_3 as secondary phase (JCPDA No. 87-1166). Y. B. Kannan *et al.*[26] have also reported the presence of α-Fe_2O_3 in Ni–Zn ferrite, which mean that these experimental conditions of calcination are not sufficient to complete the chemical reaction between the total amount of oxides. Table 2 displays the approximate crystallite size and lattice parameters of the spinel powders calcined at different calcination duration and temperatures. The strong and high intensity diffraction peak (311) was selected for the crystallite size measurement, using Scherer's equation eqn (1), were K is the shape factor of spherical particles, λ is the X-ray wavelength corresponding to Cu K_a. β denotes the full width at half-maximum of the peak in radian and θ is the Bragg's angle. Crystallite size of NZF2C2B where a double grinding and double annealing was performed, was found to be higher, with a value of 113.76 nm. The

crystallite size of the $Ni_{0.5}Zn_{0.5}Fe_2O_4$ spinel annealed at different temperatures in the range of 900 °C to 1200 °C with an increase of 100 °C has shown insignificant differences, indicating that this range of temperature exerted an insignificant influence on the crystal growth of the spinel powders. However, the increase in the annealing temperatures from 6 h to 12 h at 1200 °C increase the crystallite size from 33.73 nm to 52.56 nm.

$$D = \frac{K\lambda}{\beta \cos(\theta)} \quad (1)$$

The relation between crystal plan distance in cubic crystal lattice and lattice parameter and Bragg equation is explained below, where a is a lattice parameter, (hkl) Miller indices and d interplanar distance.

$$a = d(h^2 + k^2 + l^2)^{1/2} \quad (2)$$

$$n\lambda = 2d \sin\theta \quad (3)$$

The lattice constant of the synthesized powder had ranged from 8.387 to 8.412 Å, which agrees with the JCPDS results.

The studied $Ni_{0.5}Zn_{0.5}Fe_2O_4$ particles crystallize in the mixed spinel structure. As a result Ni^{2+} preferentially occurs in B-octahedral sites. At A-tetrahedral and B-octahedral sites Fe^{3+} is evenly distributed. The Zn^{2+}, which is nominally substituted in place of 50% of Ni^{2+} is preferentially dispersed across the A-tetrahedral site pushing some of the Fe^{3+} ion to migrate to the B-octahedral site. Fig. 1d represents the mixed spinel ferrite unit cell generated based on the crystal structure carried out with the use of Vesta software.

3.3. Morphological properties

Morphological study of all samples is carried out with a scanning electron microscope (SEM) shown in Fig. 2. Most of the particles exhibited a non-spherical (roughly spherical) shape, consistent with findings in the literature.[27] Notably, the samples display strong agglomeration, as observed in the figure, due to interaction between the magnetic materials.[28] The level of agglomeration increased with higher temperatures and prolonged sintering times. It can be seen from the image the particles were fine and uniform, with a size of approximately 11 μm at 900 °C. As the temperature increased, the particle continued to grow and became larger. Interestingly, we found that the particle size of the sample is significantly larger than the crystallite size mentioned earlier, which is agglomerated to extent and which can be attributed to the fact that magnetic crystallites are more likely to aggregate during the regrowth to form larger particles.[29] With an increase in sintering time at constant temperature of 1200 °C, a substantial growth in particle size was observed. On the other hand, varying the milling time from 30 to 60 min had no discernible impact on particles size, as evident in samples NZF-1-6 and NZF-1-12. In conclusion, sample number 5 (NZF1200) exhibited a better distribution of particle size and morphology compared to the

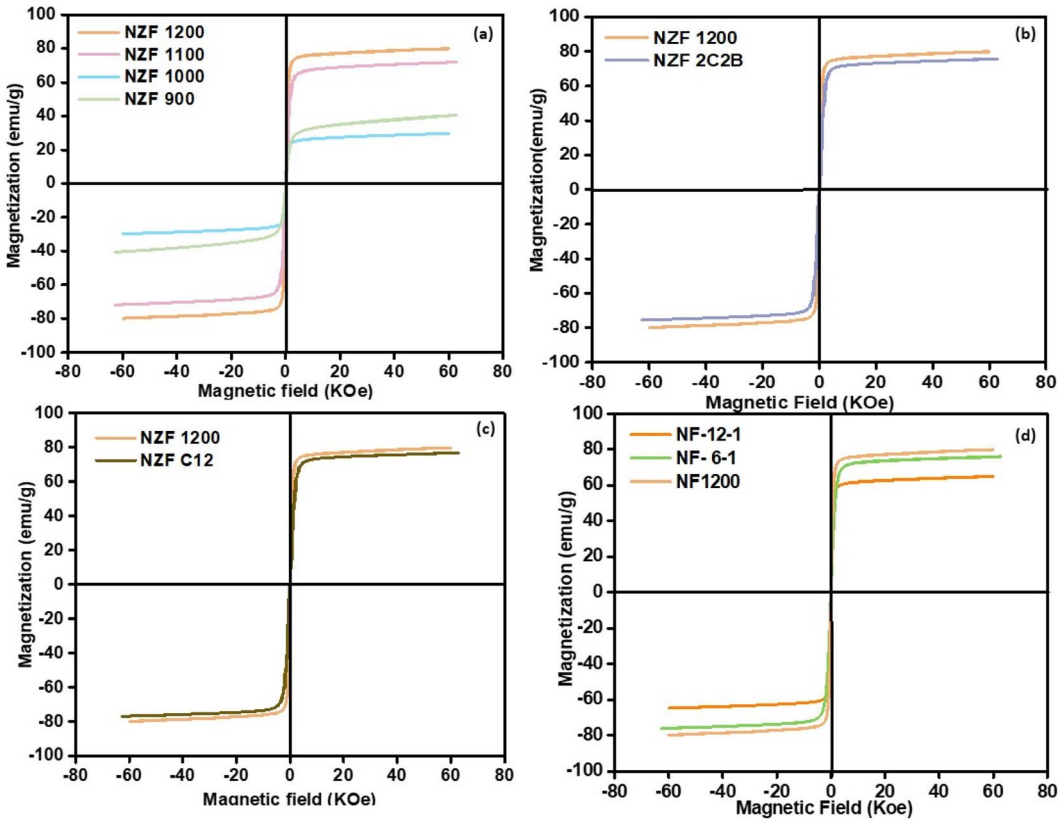

Fig. 3 Hysteresis loop of nickel zinc ferrite ($Ni_{0.5}Zn_{0.5}Fe_2O_4$) particles.

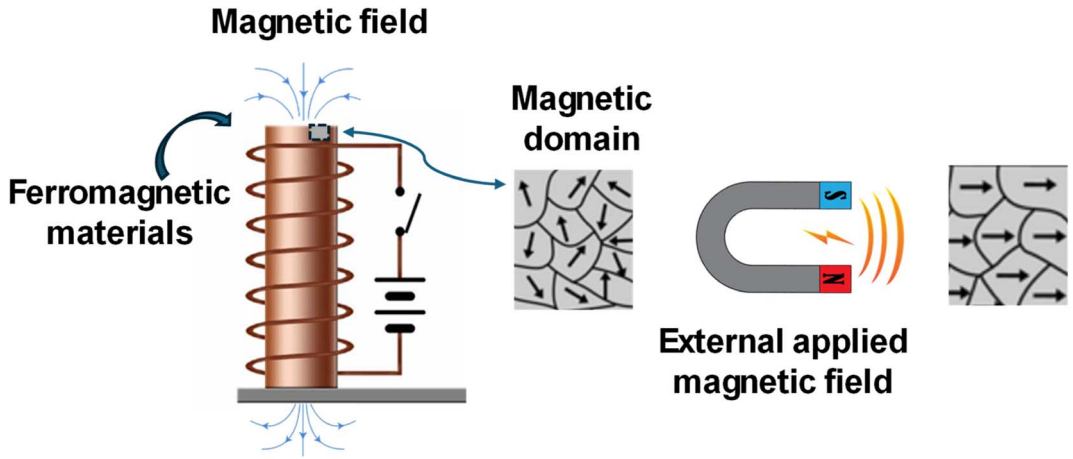

Fig. 4 Schematization of magnetic mechanisms.

other samples. The elemental composition of all the synthesized samples was studied by EDS. Energy dispersive spectroscopy (EDS) gives a useful analysis of elemental composition that can be used to determine the stoichiometry of the material. The EDS spectra of all prepared samples were shown in Fig. S1.† It was evident that the powders contained mainly Fe, Ni, and Zn. Quantitative EDS analysis result showed that the atomic percentage of metallic ions in the $Ni_{0.5}Zn_{0.5}Fe_2O_4$ has good agreement with theatrical designed stoichiometry.

3.4. Magnetic properties

The room temperature magnetic hysteresis loop of the synthesized ferrite has been measured by VSM and the results of the $Ni_{0.5}Zn_{0.5}Fe_2O_4$ samples were presented in Fig. 3. The magnetic parameters such as saturation magnetization, coercivity, and remanence of the samples are listed in Table S1.† It was found that the magnetic properties of $Ni_{0.5}Zn_{0.5}Fe_2O_4$ ferrites were related to the sintering temperature and time. All the synthesized ferrites belong to the category of soft ferrites indication low coercivity. Additionally, the coercivity was reduced with the increase of annealing temperature and time.[30,31] It is well known that coercivity is highly dependent on major parameters such as the particle size and anisotropy constant and can be also altered by heat treatment or deformation. Regarding the SEM images, the particle size is increased by increasing the time and sintering temperature and consequently influences coercivity.[32] Fig. 3a shows hysteresis loops of ferrite samples sintered at 1200, 1100, 1000, and 900 °C temperature for 6 h. It can be found from Table S1† that the saturation magnetization decreases first from 900 to 1000 °C, and then increases from 1000 to 1200 °C. This change in saturation magnetization is largely dependent on the particle size and the distribution of cations in the crystal.[33] The calcination temperature affects the distribution of Ni^{2+}, Zn^{2+}, and Fe^{3+} ions in tetrahedral (A) and octahedral (B) sites. At lower temperatures, an unfavorable cation distribution may occur, reducing magnetic interactions. As the temperature increases, more favorable cation distribution can take place, improving the magnetic properties. The initial drop in M_s value from 900 °C to 1000 °C may be due to the displacement of Zn^{2+} ions into the tetrahedral site, reducing the net magnetization. As the temperature further increases, Zn^{2+} relocates to optimal positions, enhancing the magnetic properties.[34] In addition at lower calcination temperatures (900–1000 °C), incomplete crystallization or the presence of secondary phases might occur, reducing the magnetic properties. As the calcination temperature increases, more crystalline and uniform ferrite structures are formed, improving the magnetic interactions. Between 1000 °C and 1200 °C, increased grain growth and elimination of secondary phases enhance the magnetic properties, leading to an increase in saturation magnetization at higher temperature.[35,36] The particles size is directly proportional to magnetic domain size. As the magnetic domain size increases, the atomic spin numbers increase and align themselves in the direction of the applied magnetic field, thereby enhancing the magnetic saturation of the materials.[37] As the particles size increase with the increase of calcination temperature, SEM images showed, the size of magnetic domains increases. When magnetic domain grows, more atomic spins are involved, and they tend to align more easily with an external magnetic field. This alignment boosts the overall magnetization of the material, leading to higher saturation magnetization.[38] Fig. 3b illustrates that applying double grinding and double calcination does not exert any additional influence on the magnetic saturation M_s of the prepared material. This observation highlights that elevated M_s values ($M_s = 80.07$ emu g^{-1}) are achieved through calcination at 1200 °C, which is higher than what is reported in the literature.[39,40] From Fig. 3c and d we can conclude that milling time variation from 30 min to 60 min had no effect on magnetic properties of the samples, but the increase of calcination time from 6 h to 12 h has a great impact on M_s, which decreased with the increase of calcination time. This change on magnetic properties with the increase of calcination temperature and time is related to the increase of agglomeration, which is already discussed in SEM images, which show that for sample calcined at 1200 °C for 6 h (NZF1200) the particles are more dispersed with

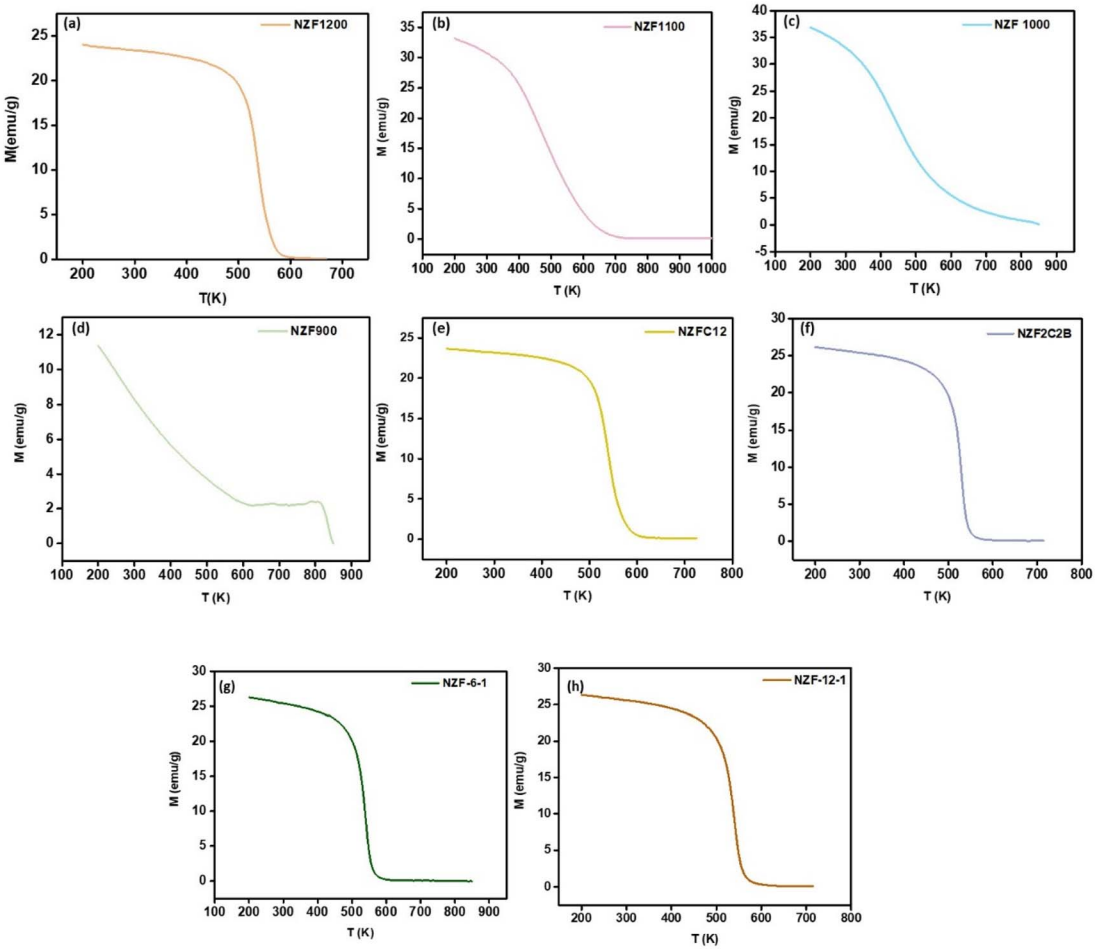

Fig. 5 Measured magnetization *versus* temperature curve of nickel zinc ferrite ($Ni_{0.5}Zn_{0.5}Fe_2O_4$) particles.

a defined shape and smooth surface. In contrast when we increase the temperature and time of calcination the agglomeration increases, since the saturation magnetization of magnetic particles is directly proportional to the number of magnetic domains and their alignment, the reduction in the number of domains due to agglomeration leads to a decrease in saturation magnetization.[35] Fig. 4 illustrate the magnetic mechanisms in ferromagnetic materials. The Curie temperature is the thermal energy required to completely destroy the magnetic interaction between neighboring magnetic ions, leading to a paramagnetic material.[41] The variation of Curie temperature T_c is presented in Fig. 5 which show an increase with the increase of sintering temperature due to the increase in particle size, and structural parameters Table S1.† By decreasing the lattice parameters, the distance between the interacting ions in the A and B sites decreases and as a result, the power of interactions increases. Therefore, the thermal energy required to offset the alignment of magnetic moment increases which lead to an increase in Curie temperature.[42]

4. Conclusion

To conclude, this study focused on the optimization of low-energy-solid-state-reaction parameters to reduce the energy consumption in the fabrication of magnetic materials, and to achieve optimal particles size and shape of magnetic fillers in polymers matrices, thus producing magnetic polymers composites materials. The synthesis of $Ni_{0.5}Zn_{0.5}Fe_2O_4$ ferrite magnetic particles *via* solid-state reaction was successfully achieved. XRD analysis revealed that temperature significantly influences the purity of the spinel structure, with all samples exhibiting a single-phase spinel structure at temperatures above 1000 °C. Despite the non-spherical morphology of the particles, the absence of impurities indicates the effectiveness of the synthesis method. Furthermore, both particle size and agglomeration levels increased with higher calcination temperatures and longer durations. The magnetic properties of ferrite particles, characterized by low coercivity and high saturation magnetization, were found to be closely linked to the sintering condition. Specifically, the sample synthesized at 1200 °C for 6 hours exhibited the highest saturation magnetization value of 80.07 emu g^{-1}, with uniform particle size and shape. Thus, the optimal condition conditions of solid-state reaction synthesis are identified as 30 minutes of mixing and the calcination temperature of 1200°c for 6 hours, resulting in a pure spinel structure with desirable morphology and enhanced magnetic properties. These characteristics make

them excellent fillers material for polymer matrices, leading to high-performance magnetic polymer composite materials.

Data availability

The data that support the findings of this study are available from the corresponding author, Mounir El Achaby, upon reasonable request.

Conflicts of interest

There are no conflicts to declare.

Acknowledgements

This research receives support from the Moroccan Ministry of Higher Education, Scientific Research, and Innovation, along with funding from the OCP Foundation through the APRD research program.

References

1 Q. Li, *et al.*, Electrostatically fabricated heterostructure of interfacial-polarization-enhanced Fe3O4/C/MXene for ultra-wideband electromagnetic wave absorption, *J. Colloid Interface Sci.*, 2024, **662**, 796–806.
2 A. Anagha, *et al.*, Structural, optical and magnetic properties of MgFe2O4 and Ni0.5Zn0.5Fe2O4, *Mater. Chem. Phys.*, 2024, **313**, 128746.
3 Y. Chen and Y. Wang, Integrating Sulfur Doping with a Multi-Heterointerface Fe_7S_8/NiS@C Composite for Wideband Microwave Absorption, *Small*, 2024, **20**(36), e2401618.
4 K. Nan, *et al.*, Integrated design of MOFs-derived 0D/1D/2D/3D hierarchical network for high-efficiency electromagnetic wave absorption, *Carbon*, 2024, **224**, 119049.
5 T. J. Shinde, A. B. Gadkari and P. N. Vasambekar, Magnetic properties and cation distribution study of nanocrystalline Ni-Zn ferrites, *J. Magn. Magn. Mater.*, 2013, **333**, 152–155.
6 A. Bajorek, Microstructural and magnetic characterization of $Ni_{0.5}Zn_{0.5}Fe_2O_4$ ferrite nanoparticles, *J. Phys. Chem. Solids*, 2019, 1–12.
7 A. S. Fawzi, A. D. Sheikh and V. L. Mathe, Structural, dielectric properties and AC conductivity of Ni (1-x) ZnxFe2O4 spinel ferrites, *J. Alloys Compd.*, 2010, **502**, 231–237.
8 R. K. Singh, C. Upadhyay, S. Layek and A. Yadav, Cation distribution of Ni0.5Zn0.5Fe2O4 nanoparticles, *Int. J. Eng. Sci. Technol.*, 2010, **2**, 104–109.
9 S. Hasan and B. Azhdar, Effect of annealing temperature, annealing time, and hydrogen potential on the physical properties of Ni0.5Zn0.5Fe2O4 nanoparticles, *Ceram. Int.*, 2023, **49**, 5371–5381.
10 N. H. Abdullah, M. S. Mustaffa, M. N. Hamidon, F. N Shafie, I. Ismail, I. R Ibrahim, *et al.*, Isochronal recovery behaviour on electromagnetic properties of polycrystalline nickel zinc ferrite (Ni0.5Zn0.5Fe2O4) prepared via mechanical alloying, *Sci. Rep.*, 2021, **11**, 1–11.
11 P. Gao, *et al.*, Structural investigations and magnetic properties of sol-gel Ni0.5Zn0.5Fe2O4 thin films for microwave heating, *J. Appl. Phys.*, 2010, **107**, 8.
12 B. S. Yoo, *et al.*, Effects of solution concentration on the structural and magnetic properties of Ni0.5Zn0.5Fe2O4 ferrite nanoparticles prepared by sol-gel, *J. Magn.*, 2013, **18**, 230–234.
13 L. Ben Tahar, M. Jaip, A. Abd, E. Abualreish and A. Noubigh, Optimization of reaction variables in the sol-gel synthesis of Ni0.5Zn0.5Fe2O4 nanoparticles as a very fast adsorbent of methylene blue, *Desalin. Water Treat.*, 2024, **317**, 100052.
14 S. Kumar, V. Singh, S. Aggarwal, U. K. Mandal and R. K. Kotnala, Synthesis of nanocrystalline Ni0.5Zn0.5Fe2O4 ferrite and study of its magnetic behavior at different temperatures, *Mater. Sci. Eng. B*, 2010, **166**, 76–82.
15 A. Bajorek, *et al.*, Microstructural and magnetic characterization of Ni0.5Zn0.5Fe2O4 ferrite nanoparticles, *J. Phys. Chem. Solids*, 2019, **129**, 1–21.
16 V. D. Sudheesh, *et al.*, Investigation of structural and magnetic properties of Ni0.5Zn0.5Fe2O4 nano powders prepared by self combustion method, *Mater. Res. Bull.*, 2013, **48**, 698–704.
17 H. Aali, *et al.*, High antibacterial and photocatalytic activity of solution combustion synthesized Ni0.5Zn0.5Fe2O4 nanoparticles: effect of fuel to oxidizer ratio and complex fuels, *Ceram. Int.*, 2019, **45**, 19127–19140.
18 N. Wang, *et al.*, Two-phase magnetic nanospheres with magnetic coupling effect encapsulated in porous carbon to achieve lightweight and efficient microwave absorbers, *J. Colloid Interface Sci.*, 2024, **671**, 56–66.
19 M. Zhang, *et al.*, Porous Ni0.5Zn0.5Fe2O4 Nanospheres: Synthesis, Characterization, and Application for Lithium Storage, *Electrochim. Acta*, 2014, **147**, 143–150.
20 Y. M. Kwon, M. Y. Lee, M. Mustaqima, C. Liu and B. W. Lee, Structural and magnetic properties of Ni0.6Zn0.4Fe2O4 ferrite prepared by solid state reaction and sol-gel, *J. Magn.*, 2014, **19**, 64–67.
21 T. F. Marinca, I. Chicinas, O. Isnard, V. Pop and F. Popa, Synthesis, structural and magnetic characterization of nanocrystalline nickel ferrite - NiFe2O4 obtained by reactive milling, *J. Alloys Compd.*, 2011, **509**, 7931–7936.
22 C. A. Palacio Gómez, C. A. Barrero Meneses and A. Matute, Structural parameters and cation distributions in solid state synthesized Ni-Zn ferrites, *Mater. Sci. Eng. B*, 2018, **236–237**, 48–55.
23 S. Baayyad, *et al.*, High-density polyethylene composites filled with micro- and nano-particles of nickel ferrite: magnetic, mechanical, and thermal properties, *RSC Adv.*, 2024, **14**, 18750–18763.
24 A. Damnjanović and N. Kovačević, Influence of Magnet Particle Shape on Magnetic and Environmental Stability of FDM Polymer-Bonded Magnets, *Materials*, 2023, **16**, 2993.
25 *Mechanisms and Reactions in the Solid State*, pp. 129–189.

26 Y. B. Kannan, R. Saravanan and N. Srinivasan, Sintering effect on structural, magnetic and optical properties of $Ni_{0.5}Zn_{0.5}Fe_2O_4$ ferrite nano particles, *J. Magn. Magn. Mater.*, 2017, **423**, 217–225.

27 S. M. Yasin, Superparamagnetic Ni0.5Zn0.5Fe2O4 nanoparticles prepared by ball-milling, *Appl. Phys. A: Mater. Sci. Process.*, 2023, **129**, 24–27.

28 R. V. Bharathi, *et al.*, Enhanced DC electrical resistivity and magnetic properties of transition metal cobalt substituted spinel MgFe2O4 ferrite system, *Inorg. Chem. Commun.*, 2023, **158**, 111713.

29 C. Chen, Y. Yang, D. Chen, Y. Zhang and Y. Meng, Micro-structural and magnetic analysis of spinel high entropy oxides synthesized by two-step pressureless sintering provides insight into high entropy ceramics, *Mater. Today Commun.*, 2023, **35**, 106122.

30 S. Akhter, *et al.*, Magnetic Properties of Cu1-xZnxFe2O4 Ferrites with the Variation of Zinc Concentration, *J. Mod. Phys.*, 2012, **03**, 398–403.

31 B. Shahbahrami, S. M. Rabiee, R. Shidpour and H. Salimi-Kenari, Influence of calcination parameters on the microstructure, magnetic and hyperthermia properties of Zn-Co ferrite nanoparticles, *J. Electroceram.*, 2022, **48**, 157–168.

32 A. Ghasemi and M. Mousavinia, Structural and magnetic evaluation of substituted NiZnFe2O4 particles synthesized by conventional sol-gel method, *Ceram. Int.*, 2014, **40**, 2825–2834.

33 Y. Han, A. Sun, X. Pan, W. Zhang and X. Zhao, Effect of Different Sintering Temperatures on Structural and Magnetic Properties of Zn–Co Ferrite Nanoparticles, *J. Supercond. Nov. Magnetism*, 2019, **32**, 3823–3830.

34 H. Nikmanesh, M. Eshraghi and S. karimi, Cation distribution, magnetic and structural properties of CoCrxFe2-xO4: Effect of calcination temperature and chromium substitution, *J. Magn. Magn. Mater.*, 2019, **471**, 294–303.

35 S. M. Olhero, *et al.*, Co-precipitation of a Ni-Zn ferrite precursor powder: Effects of heat treatment conditions and deagglomeration on the structure and magnetic properties, *J. Eur. Ceram. Soc.*, 2012, **32**, 2469–2476.

36 B. Purnama, A. T. Wijayanta and Suharyana, Effect of calcination temperature on structural and magnetic properties in cobalt ferrite nano particles, *J. King Saud Univ. Sci.*, 2019, **31**, 956–960.

37 S. J. Olusegun, E. T. F. Freitas, L. R. S. Lara, H. O. Stumpf and N. D. S. Mohallem, Effect of drying process and calcination on the structural and magnetic properties of cobalt ferrite, *Ceram. Int.*, 2019, **45**, 8734–8743.

38 I. Panneer Muthuselvam and R. N. Bhowmik, Mechanical alloyed Ho3+ doping in CoFe2O4 spinel ferrite and understanding of magnetic nanodomains, *J. Magn. Magn. Mater.*, 2010, **322**, 767–776.

39 K. Kim, K. W. Jeon, K. W. Moon, M. K. Kang and J. Kim, Effects of Calcination Conditions on Magnetic Properties in Strontium Ferrite Synthesized by the Molten Salt Method, *IEEE Trans. Magn.*, 2016, **52**, 8–11.

40 R. Masrour, *et al.*, Synthesis and magnetic properties of bulk ferrites spinels Ni0.5Zn0.5Fe2O4: Experimental an Ab-initio study, *J. Supercond. Nov. Magnetism*, 2014, **27**, 177–181.

41 H. Huili, B. Grindi, G. Viau and L. Ben Tahar, Effect of cobalt substitution on the structure, electrical, and magnetic properties of nanorcrystalline Ni0.5Zn0.5Fe2O4 prepared by the polyol process, *Ceram. Int.*, 2014, **40**, 16235–16244.

42 X. Pan, A. Sun, Y. Han, W. Zhang and X. Zhao, Effects of different sintering temperature on structural and magnetic properties of Ni-Cu-Co ferrite nanoparticles, *Mod. Phys. Lett. B*, 2018, **32**, 1067–1076.